JOURNAL OF MATERIALS SCIENCE **40** (2005) 3031 – 3034 LETTERS

Preparation and characterization of α-FeOOH and α-Fe_2O_3 by sol–gel method

M. A. DAR
Thin Film Technology Laboratory, School of Chemical Engineering, Chonbuk National University, Chonju 561-576, Republic of Korea

S. K. KULKARNI
Department of Physics, University of Pune, Ganeshkhind, Pune 411007, India

Z. A. ANSARI, S. G. ANSARI
School of Materials Science, Japan Advanced Institute of Science and Technology, 1-1, Asahidai, Tatsunokuchi, Ishikawa 923-1292, Japan

HYUNG-SHIK SHIN*
Thin Film Technology Laboratory, School of Chemical Engineering, Chonbuk National University, Chonju 561-576, Republic of Korea
E-mail: hsshin@chonbuk.ac.kr

There is an everincreasing interest in materials with reduced dimensions. Materials may be metals, metal oxides, semiconductors, insulators, etc. The major aim of the nanoparticles research is to synthesize the controlled particles in large quantities and understand their properties before using them for any application. It is observed that below a critical size, which is characteristic of that material, various physicochemical properties start changing dramatically. These critical dimensions are in the range of a nanometer to few hundreds of nanometer. To generate colloidal particles of narrow size distribution (d), the nucleation and growth processes must be precisely controlled. A large number of reports on synthesis of oxide particles as well as studies on their growth are available [1–6].

The study of nanoparticles has received increasing attention recently. Reduction of the particle size to the nanometer range results in the altered electrical, magnetic, electro-optical, and chemical properties [7–9]. Earlier reports indicate that the crystallization of α-FeOOH particles was inhibited in the presence of both anions and the size of α-FeOOH particles was decreased with increased concentration of the added anions [10]. Cornell and Giovanoli investigated the phase transformation of β-FeOOH to α-FeOOH and/or α-Fe_2O_3 in an alkaline medium [11]. It is generally accepted that the phase transformation from β-FeOOH to α-FeOOH to α-Fe_2O_3 occurs via the dissolution/precipitation mechanism [12]. It is reported that without mineralizer, the transformation α-FeOOH to α-Fe_2O_3 takes place under hydrothermal conditions at moderate temperature (∼200 °C) [13]. Indeed, the effect of nanoscale confinement originates the unusual magnetic behavior which may strongly differ, from those observed on conventional bulk materials, in several aspects. In addition to theoretical reasons, the engineering of nanoscale materials has become a very challenging technology, for example in the information storage and data processing with increasing density [14]. It is to be noted that the surface area and chemical reactivity of nanosized particles are much higher than the conventional bulk material [16–19]. The sol–gel process has the unique advantage of producing large-surface area films at low cost [20, 21].

In this paper, the sol–gel method is used to produce α-FeOOH and α-Fe_2O_3 particles in the nanometric form with large surface area. Iron-oxide nanoparticles were prepared by dissolving 4.04 g (0.05 M) of $Fe(NO_3)_3 9H_2O$ into 1000 ml double-distilled water to which 1 M of NaOH was added under stirring until the pH was raised to 13.1. The resulting brown precipitate $\{Fe(OH)_3\}$ was washed with double-distilled water and supernatant liquid was decanted. The procedure was repeated 10–15 times to achieve the pH of ∼7.1. The same procedure was applied for all samples. The $FeCl_3$ was obtained by the dropwise addition of HCl (1 M) to the solution, followed by the addition of NaH_2PO_4 (0.1 M). The remaining solution was filled up with double-distilled water to 1000 ml and was kept for 72 hr at 100 ± 5 °C in a closed flask. The precipitate was dried out at 100 °C in an oven for 1 hr to get α-FeOOH. When the same product was dried at a higher temperature (200–300 °C) for 3 hr, it led to α-Fe_2O_3. The powder could readily be resuspended in the aqueous solution of desired pH in an ultrasonic bath.

The reactions during the synthesis of α-FeOOH and α-Fe_2O_3 are summarized in Scheme 1. Characterization was carried out using various techniques. The phases and size of particles were identified and measured by X-ray diffraction (XRD) measurement (Philips PW 1840 powder X-ray diffractometer) with Fe K_α as the source of incident radiation, and Bragg

---

*Author to whom all correspondence should be addressed.

0022–2461

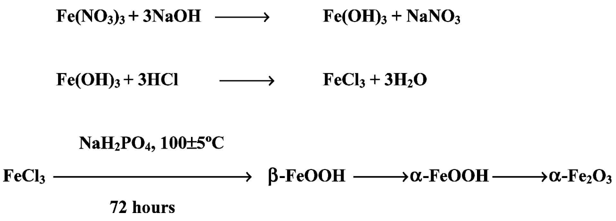

$$Fe(NO_3)_3 + 3NaOH \longrightarrow Fe(OH)_3 + NaNO_3$$

$$Fe(OH)_3 + 3HCl \longrightarrow FeCl_3 + 3H_2O$$

$$FeCl_3 \xrightarrow[\text{72 hours}]{NaH_2PO_4,\ 100\pm5^{\circ}C} \beta\text{-}FeOOH \longrightarrow \alpha\text{-}FeOOH \longrightarrow \alpha\text{-}Fe_2O_3$$

Scheme 1 The reaction taking place during the synthesis of α-FeOOH and α-Fe_2O_3.

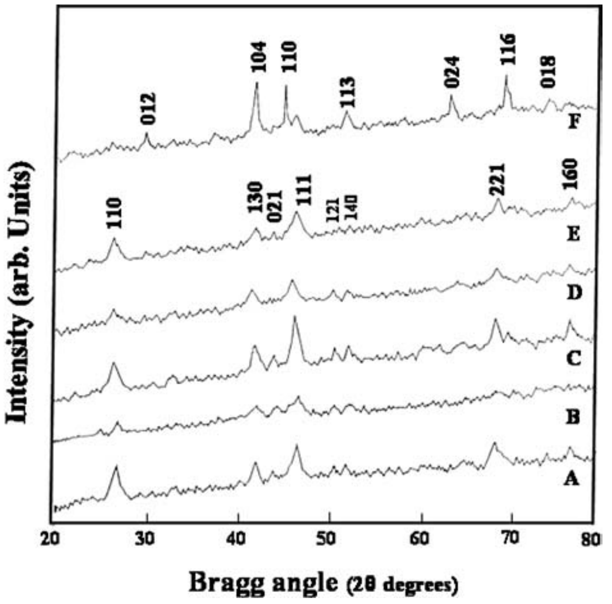

Figure 1 X-ray diffraction patterns of Samples A to E (indicating α-FeOOH phase) and of Sample F (indicating α-Fe_2O_3 phase).

angle ranges from 20 to 80 °. The morphology of the samples was investigated by using Scanning electron microscope (Lieca-Cambridge Steroscan S-440). The surface area of the solid material was measured from Brunaur-Emmett-Teller (BET) analysis. Time of Transition Theory was used to measure the particle size distribution.

The X-ray diffraction spectra of α-FeOOH and α-Fe_2O_3 with pH variations are presented in Fig. 1 and the corresponding pH values and particle sizes are listed in Table I respectively. The average particle size is estimated using Scherrer formula. It is realized from Fig. 1 and Table I that the increasing pH of the sample (A–F) results in the decrease of particle size, which is evident by the changes in peak width (broadness and narrowness). It can be clearly seen that the variation of particle size with pH values is in good agreement with the broadening of XRD peaks. This indicates that the pH has an important role in the size of the particles. The elemental analysis shows that the samples A–E (Fig. 1) correspond to α-FeOOH phase only. The peaks corresponding to α-Fe_2O_3 were not observed. Whereas in case of Sample F, only Hematite phase (α-Fe_2O_3) is observed, which is due to the decomposition of α-FeOOH into α-Fe_2O_3 on heating at 200–300 °C [22].

TABLE I Size of particles of Samples A–F with corresponding pH

Sample no.	Sample pH	pH variation	Particle size (nm)
A	13.1	7.1	7.4
B	12.0	8.2	9.0
C	12.9	8.7	8.1
D	12.56	8.7	9.0
E	12.0	8.7	10.2
F	10.35	8.7	20.6

The samples for morphological studies using Scanning Electron Microscope were prepared by spin-coating technique. For isolating Fe_2O_3 particles, organic solvent was added to the powder and was then kept in an ultrasonic bath for 10 min. The scanning images (Fig. 2) of the samples (A, B, D, and E) show a uniform distribution of the size and shape of the particles in a sample. The average lengths and widths of the agglomerate α-FeOOH, listed in Table II, are in nanometer range. The effect of the pH variation can also be seen in these images, which affects the size, shape, and morphology of the particles. In SEM photographs, we can observe the agglomeration of particles; this is mainly due to the annealing of sample at 100 °C.

The size distribution of Sample F (α-Fe_2O_3) was carried out by Time of Transition Theory method (CIS-100). In Fig. 3 the sharpness of the peak indicates that all particles in the sample (F) are in uniform distribution. The sample was sonicated for 1200 s to avoid aggregation of particles. The average particle size was found to be ~80 nm with 1.57 polydispersity. The specific surface area "S" of the solid was calculated from the total surface area "S_t" and the sample weight "W," using the following equation;

$$S = S_t/W \tag{1}$$

The specific surface area was calculated for all samples and is given in Table III. The effect of pH on the samples can be seen here too i.e. when the pH increases, the specific surface area also increases.

In conclusion, iron-oxide particles were synthesized by the sol–gel method. X-ray diffraction analysis shows two phases corresponding to α-FeOOH and α-Fe_2O_3.

TABLE II Shape of the particles of Samples A, B, D, and E with corresponding pH

Sample no.	Sample pH	Average length (nm)	Average width (nm)	Shape
A	13.1	226	87	Elongated
B	12.0		75	Spherical/agglomerated
D	12.56	232	62	Elongated
E	12.0		86	Spherical

TABLE III Specific surface area of the particles with pH variation and size

Sample no.	pH variation	Sample pH	Size (nm)	Sp. surfcae area
A	7.1	13.1	7.4	198
B	8.4	12.0	9.0	168
D	8.7	12.56	9.0	126
E	8.7	12.0	10.2	98
F	8.7	10.35	20.6	40

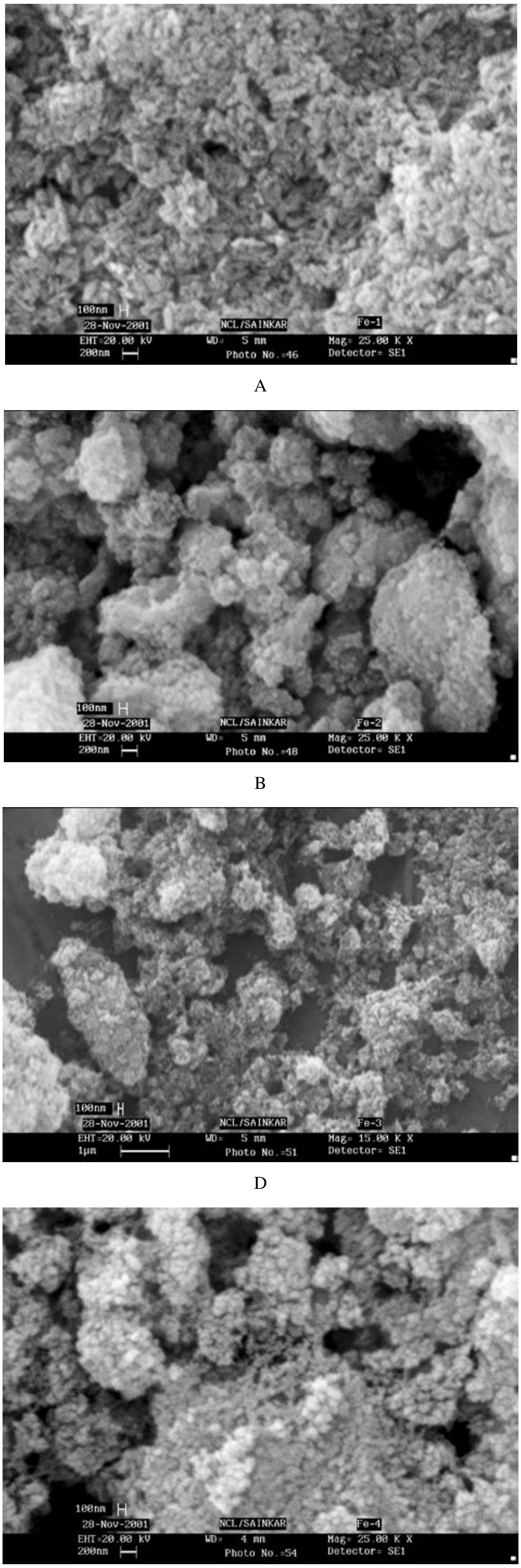

A

B

D

E

Figure 2 SEM micrographs of the samples (A) pH = 13.1, (B) pH = 12, (D) pH = 12.56, and (E) pH = 12.

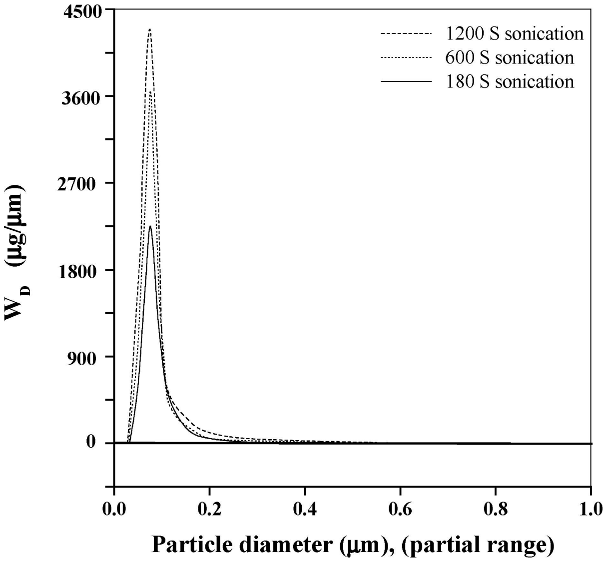

Figure 3 Particle size distribution of α-Fe_2O_3 (F), measured using Time of Transition theory.

Particle size measurement from XRD patterns shows that the particle size decreases with increasing pH. Morphological study of all samples reveals uniform size and shape distribution in a sample. With increasing pH, the shapes of the particles change randomly from spherical to elongated grains. BET analysis shows that increasing pH of the sample results in increase in the specific surface area. Hence we can conclude that the pH has an important role in size, morphology, and specific surface area of the samples. In addition to this, the concentration of $Fe(NO_3)_3$, pH of the reaction, aging period, and NaH_2PO_4 solution play an important role in the morphology of the precipitated particles.

Acknowledgments

M. A. Dar wishes to acknowledge the graduate fellowship from Korean Science and Engineering Federation; Korea. Z. A. Ansari and S. G. Ansari acknowledges the post doc fellowship from JSPS, Japan.

References

1. E. MATIJEVIC and P. SCHEINER, *J. Coll. Interf. Sci.* **63** (1978) 509.
2. T. SUGIMOTO and E. MATIJEVIC, *ibid.* **74** (1980) 227.
3. H. TAMURA and E. MATIJEVIC, *ibid.* **90** (1982) 100.
4. M. OZAKI, S. KRATOHVIL and E. MATIJEVIC, *ibid.* **102** (1984) 146.
5. P. BELLEVILLE, J. JOLIVET, E. TRONC and J. LIVAGE, *ibid.* **150** (1992) 453.
6. N. RYDE, H. KIHIRA and E. MATIJEVIC, *ibid.* **151** (1992) 421.
7. T. TAKAGAHARA and E. HANAMURA, *Phys. Rev. Lett.* **56** (1986) 2553.
8. C. FLYTZANIS, *J. Opt. Soc. Am. B* **4** (1987) 6.
9. L. E. BRUS, *J. Phys. Chem.* **80** (1984) 4403.
10. A. SARIC, S. MUSIC, K. NOMURA and S. POPOVIC, *Mater. Sci. Engng. B* **56** (1998) 43.
11. S. MUSIC, G. P. SANTANA, G. SMIT and V. K. GARG, *J. Alloys Comp.* **278** (1998) 291.
12. S. MUSIC, I. CZAKO-NAGY, I. SALAJ-OBELIC and N. LJUBESIC, *Mater. Lett.* **32** (1997) 301.

13. L. DIAMANDESCU, D. MIHAILA-TARABASANU and N. POPESCU-POGRION, *ibid.* **27** (1996) 253.
14. S. MORUP, J. A. DUMESIC, H. TOPSOE and R. L. COHEN (ed.), in “Applications of Mossbaur Spectroscopy” (Academic Press, New York, 1980) p. 1.
15. G. D. STUCKY and J. E. MACDOUGALL, *Science* **247** (1990) 669.
16. V. V. KRESIN, *Phys. Rep.* **220** (1992) 1.
17. X. CAO, Y. KOLTYPIN, R. PROZOROV, G KATABI and A. GEDANKEN, *J. Mater. Chem.* **7** (1997) 2447.
18. Z. BOWEN, *Phys. D* **26** (1993) 46.
19. S. S. PARK, H. X. ZHENG and J. D. M ACKENZIE, *Mater. Lett.* **17** (1993) 346.
20. A. WILSON, J. D. WRIGHT and J. J. MURPHY, *Sens. Actuat. B* **18/19** (1994) 506.
21. M. OZAKI, S. KRATOHVIC and E. MATIJEVIC, *J. Coll. Interf. Sci.* **102** (1984) 146.
22. H. NAONO and R. FUJIWARA, *ibid.* **73** (1980) 406.

Received 24 February
and accepted 26 August 2004